

# Pharmacokinetics in Rat of P8, a Peptide Drug Candidate for the Treatment of Alzheimer's Disease: Stability and Delivery to the Brain<sup>1</sup>

Nazneen N. Dewji<sup>a,b,\*</sup>, Marc R. Azar<sup>c</sup>, Leah R. Hanson<sup>d</sup>, William H. Frey II<sup>d</sup>,  
Bruce H. Morimoto<sup>e</sup> and David Johnson<sup>f</sup>

<sup>a</sup>*Cenna Biosciences Inc., La Jolla, CA, USA*

<sup>b</sup>*Department of Medicine, UC San Diego, La Jolla, CA, USA*

<sup>c</sup>*Behavioral Pharma, La Jolla, CA, USA*

<sup>d</sup>*HealthPartners Institute, St. Paul, MN, USA*

<sup>e</sup>*Celerion Inc., USA*

<sup>f</sup>*Microconstants LLC, San Diego, CA, USA*

Accepted 25 August 2018

**Abstract.** Strategies to achieve a therapy for Alzheimer's disease (AD) aimed at reducing the effects of amyloid- $\beta$  (A $\beta$ ) have largely involved inhibiting or modifying the activities of the  $\beta$ - or  $\gamma$ -secretases or by the use of monoclonal antibodies (MAb). We previously offered the potential for a new, early and effective approach for the treatment of AD by a strategy that does not target the secretases. We showed that a family of peptides containing the DEEEDEEL sequence and another independent peptide, all derived from the amino terminus of PS-1, are each capable of markedly reducing the production of A $\beta$  *in vitro* and in mThy1-hAPP transgenic mice. These peptides gave a strong and specific binding with the ectodomain of amyloid- $\beta$  protein precursor (A $\beta$ PP) and did not affect the catalytic activities of  $\beta$ - or  $\gamma$ -secretase, or the level of A $\beta$ PP. Critical to the development of any therapeutic for AD is the requirement that it is stable and can be delivered to the brain. We report here data on the metabolic stability and delivery to the rat brain of our lead candidate P8 by intravenous (IV), intranasal (IN), and subcutaneous (SC) administration. Pharmacokinetics (PK) of P8 in rat plasma and CSF following a single dose of P8 demonstrate that SC administration gives better absorption compared to IN and is the delivery method of choice for the further development of P8 as a clinical candidate.

**Keywords:** Alzheimer's disease, amyloid- $\beta$ , A $\beta$ , amyloid- $\beta$  protein precursor, presenilin, peptide drug, pharmacokinetic

## INTRODUCTION

The number of individuals diagnosed with Alzheimer's disease (AD) is expected to triple by

the year 2050. There is therefore an urgent need for disease-modifying therapies that can prevent the onset or arrest the progression of the disease. Amyloid- $\beta$  (A $\beta$ ), a 39–43 amino acid fragment of the amyloid- $\beta$  protein precursor, A $\beta$ PP [1, 2] is widely recognized to be the primary neurotoxic agent in AD [3, 4]. Critically involved in the formation and release of A $\beta$  from its precursor is the action of the Presenilin proteins, PS-1 or PS-2, as part of a complex

<sup>1</sup>Dedicated to S. Jonathan Singer (1924–2017).

\*Correspondence to: Dr. Nazneen Dewji, Cenna Biosciences Inc., 505 Coast Boulevard, Suite 302, La Jolla, CA 92037, USA.  
Tel.: +1 858 456 0821; E-mail: ndewji@cennabiosciences.com.

of other proteins [5, 6]. Strategies to date to achieve a therapy for AD aimed at reducing the effects of A $\beta$  have largely involved inhibiting or modifying the activities of the  $\beta$ - or  $\gamma$ -secretases or by the use of monoclonal antibodies (MAb) against A $\beta$ . Attempts at inhibiting total A $\beta$  production by directly targeting the catalytic activities of these enzymes have failed due to off-target effects as both enzymes are known to hydrolyze numerous other substrates besides A $\beta$ PP.  $\gamma$ -secretase, in particular, acts upon many Type I membrane proteins [7], including Notch to yield the Notch intracellular domain (NICD) that has critically important cellular functions [8]. Although some recent  $\gamma$ -secretase modulation studies have successfully spared Notch function [9, 10],  $\gamma$ -secretase has over 50 known substrates [7], any of whose functions could potentially be undesirably affected by enzyme modulation.  $\beta$ -secretase inhibitors have entered clinical trials because they have so far proved to be less toxic than the  $\gamma$ -secretase inhibitors, but it is not known what the effects of inhibiting over 50 reactions in the cell for greater than 20 years of chronic use, will have. Data are already emerging on toxicity issues with some BACE-1 inhibitors. Johnson and Johnson have just announced that they have stopped their program on the BACE-1 inhibitor atabecostat due to liver safety issues [11]. Similarly, Merck ended Phase III studies of their BACE-1 inhibitor verubecestat after concluding that the inhibitor was unlikely to exhibit a positive benefit/risk ratio [12]. New therapeutic approaches that can inhibit total A $\beta$  production without targeting the activities of the  $\beta$ - or the  $\gamma$ -secretase are therefore of great interest.

Our previous work [13] offers the potential for a new, early, and effective approach for the treatment of AD, by a strategy that does not target the secretases. We showed first that a family of peptides containing the DEEED EEL sequence (P6, P7, and P8) and another independent peptide (P4), all derived from the amino terminus of PS-1 are each capable of markedly reducing the production of total A $\beta$  and of A $\beta$ <sub>40</sub> and A $\beta$ <sub>42</sub> *in vitro* and in mThy1-hAPP Tg mice. Second, we showed using biolayer interferometry for those peptides that were effective in reducing A $\beta$ , of a strong, specific, and biologically relevant binding with the ectodomain of human A $\beta$ PP. This binding was further confirmed by confocal microscopy for cell-surface-expressed A $\beta$ PP in fibroblasts. Finally, we demonstrated that the reduction of A $\beta$  by the peptides did not affect the catalytic activities of  $\beta$ - or  $\gamma$ -secretase, or the level of A $\beta$ PP.

Critical to the development of any therapeutic for AD is the requirement that it is stable and can be delivered to the brain. We report here results of metabolic stability studies of our lead candidate P8 in human and mouse plasma and brain extracts and two independent studies to demonstrate that it can be delivered to the rat brain. The first shows the delivery to and distribution of radiolabeled P8 in the rat brain. The second shows the pharmacokinetics (PK) of P8 in rat plasma and cerebrospinal fluid (CSF) following a single dose of P8 by intravenous (IV), intranasal (IN), and subcutaneous (SC) administration.

## MATERIALS AND METHODS

### *P8 peptide*

P8 peptide (sequence: DEEED EEL) was synthesized by Polypeptide Laboratories (Torrance CA). Identity and purity were verified by analytical HPLC. The peptide purity was greater than 99%, water content was 3.89% and sodium content was less than 0.003%.

### *Animals*

Male Sprague-Dawley (SD) rats (249–274 g, purchased from Charles River) were used in all the studies. Rats were ordered un-cannulated (for the radiolabel study) or cannulated in the jugular vein and with intra-cisternal cannulation for CSF sampling for PK studies. Animals were handled in accordance with the current NIH guidelines regarding the use and care of laboratory animals, and all applicable local, state, and federal regulations and guidelines.

### *Plasma stability studies*

An aliquot of mouse or human plasma (990  $\mu$ L) or mouse or human brain homogenate (1:3 brain:PBS, w/v; 495  $\mu$ L) was added to separate glass test tubes. To each tube was added 100  $\mu$ M P8 in methanol to a final concentration of 1  $\mu$ M in matrix. After 15 and 30 min, 1, 2, and 4-h incubation periods at room temperature, matrix proteins were precipitated with 3 mL of methanol (1.5 mL for mouse brain homogenate). The supernatant was transferred to a fresh tube, evaporated and samples were reconstituted in 0.1% formic acid in water. The reactions were analyzed using LC/MS/MS. Each time point was prepared in duplicate. Time zero samples were pre-quenched with methanol prior to the addition of P8.

### *Radiolabel distribution study*

Adult male SD rats ( $n=12$ , mean weight 315 g) were housed in pairs with free access to food and water with 12-h light cycles. Animals were split into two groups; those receiving compound by IN delivery and those receiving compound by intravenous IV delivery. After being anesthetized with a cocktail (0.7 mL/kg) consisting of 150 mg ketamine (100 mg/ml), 30 mg xylazine (20 mg/ml), and 5 mg acepromazine (10 mg/ml). IV animals underwent jugular and femoral vein cannulation and IN animals underwent jugular vein cannulation. All animals received 0.5 mg P8 and the same concentration of  $^3\text{H}$  (60  $\mu\text{Ci}$ ). All dose-solutions were made up to 60  $\mu\text{L}$ .  $^3\text{H}$ -P8 was administered by IV infusion for 18 min. Administration of  $^3\text{H}$ -P8 via IN was also completed over 18 min by delivering drops to alternating naris every 2 min while in the supine position. From this point forward, both groups were treated the same. Blood was drawn from the jugular vein at 10 and 20 min following end-of-dose administration. At 30 min, a terminal blood sample was collected via cardiac puncture prior to perfusion with saline. Brain and body tissues were also collected and processed for scintillation counting.

### *Data analysis*

P8 concentrations (nM or pmol/g tissue weight) were calculated using the weight (g) and DPM measured for each tissue sample, and the measured specific activity (pmol/DPM) of the dose administered. Mean and standard error of the mean concentration (nM or  $\mu\text{M}$ ) of each tissue sample were calculated. Any value outside two standard deviations of the mean for each tissue was considered an outlier and removed from the data set. There were no calculated outliers for this study.

### *PK study*

A single dose of P8 in PBS was administered via three routes: IV, SC, and IN. For the IV and SC routes of administration, P8 (200  $\mu\text{L}$  of a 16.5 mg/ml solution, which was equivalent to a final dose of approximately 11 mg/kg) was administered to each rat over a 1-min period. For IN administration, P8 (60  $\mu\text{L}$  of a 27.5 mg/mL solution, which was equivalent to a final dose of approximately 5.5 mg/kg) was administered to each rat by placing 10  $\mu\text{l}$  of dosing solution in each nostril (20  $\mu\text{L}$

total per administration) at 6-min intervals so that the 60  $\mu\text{l}$  was administered over an 18-min period. IN administration was carried out using a rICD Device Kit (item#1000007) manufactured by Impel NeuroPharma (kit ID:019). Following dose administration, blood samples were taken at pre-dose, 5, 15, 25, 35, 50, 70, 90, 110, 130, and 165-min from the onset of drug administration via a jugular cannula. Approximately 300  $\mu\text{l}$  of whole blood was removed and placed in  $\text{K}_2\text{EDTA}$  treated tubes and immediately placed on wet ice. The cannula was then flushed with 300  $\mu\text{l}$  of a 0.9% saline solution containing 10 units of sodium heparin. CSF (20  $\mu\text{l}$ ) was sampled at pre-dose, 10, 20, 30, 40, 60, 80, 100, 120, and 150 min via the intercisternal cannula, and wherever possible, at 180-min from the onset of drug administration. Blood was centrifuged at  $6000 \times g$  for 6.5 min and a 150  $\mu\text{l}$  aliquot of plasma was transferred to a fresh microcentrifuge tube and immediately placed on dry ice. CSF samples were placed in a microcentrifuge tube and immediately placed on dry ice. All samples were stored at  $-20^\circ\text{C}$  until analysis. PK analysis was performed using standard noncompartmental analysis models in Phoenix WinNonlin (v6.3).

### *Bioanalytical method for the detection of P8 in rat plasma and CSF*

P8 was precipitated from samples after the addition of formic acid in acetonitrile:methanol and separated by HPLC using a  $50 \times 2.1$  mm, 5  $\mu\text{m}$  Onyx monolithic C18 column. P8 was detected using a tandem quadrupole mass spectrometer (Xevo TQS, Waters, Milford, MA) using ESI in the positive mode. The parent > daughter mass transition from 1007.55 > 876.35 was used for the detection of P8. The calibration curves were obtained by fitting the log transformed peak areas against the log transformed standard concentrations using linear regression. The plasma calibration curve had a range of 1.00 to 100 ng/mL and the CSF calibration curve had a range of 0.500 to 50.0 ng/mL

### *SC administration of P8 to APPSWE Tg mice and A $\beta$ analysis*

APPSWE mice, which carry the Swedish mutation on the *APP* gene [14], were purchased from Taconic and used at 16 weeks of age. Mice ( $n=5$  per group) were administered PBS or P8 (200  $\mu\text{L}$  of a 33 mg/ml solution) subcutaneously 1X or 2X per day for 14 days after which the animals were sacrificed. The

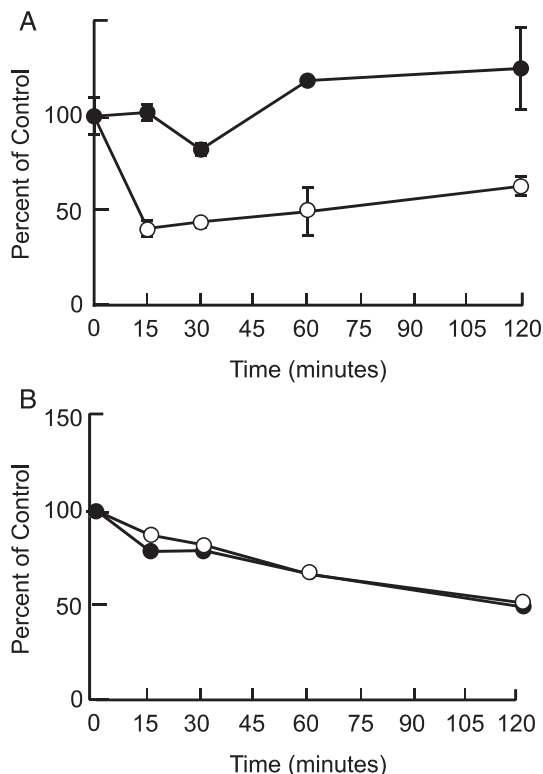


Fig. 1. Metabolic stability of P8 in mouse and human plasma (A) and brain (B). P8 (1  $\mu$ M) was added to mouse (closed circles) and human (open circles) plasma or brain extract and the reactions were incubated at room temperature for up to 4 h. The amount of P8 remaining was determined by LC/MS/MS and is presented as a percentage of the sample at time 0.

hippocampus was removed and A $\beta$ <sub>40</sub> analysis was carried out by ELISA (Invitrogen).

## RESULTS

### *Metabolic stability of P8 in mouse and human plasma and brain homogenates*

Our results showed that P8 was stable in its unmodified form in mouse and human plasma and brain homogenates. The half-life of P8 in mouse plasma was found to be >240 min; and in mouse brain homogenate was >120 min. In human plasma and brain homogenate, the half-life of P8 was >120 min. In human but not mouse plasma, there appeared to be about 50% drop in stability at around 15 min, which then stabilized and even increased slightly. This was most likely due to the non-specific binding of P8 to precipitated plasma proteins. Please see Fig. 1A, B and Table 1.

### *Delivery to the brain of <sup>3</sup>H-P8 and radiolabel distribution*

Following <sup>3</sup>H-P8 administration (497 nmol) to anesthetized rats (N = 6), radiolabel reached the CNS quickly by both IN and IV administration (Table 2 and Fig. 2). Following IV administration, radiolabel reached the brain at slightly higher concentrations (56–104 nM) than IN (36–103 nM) and was present in all parts of the brain, suggesting that P8 could reach the target once systemic exposure was achieved. As expected, animals treated intranasally with <sup>3</sup>H-P8 had higher epithelial concentrations (olfactory: 14  $\mu$ M and respiratory: 1,303  $\mu$ M) than those treated intravenously (olfactory: 0.26  $\mu$ M and respiratory: 0.28  $\mu$ M). The lower concentration of P8 in the olfactory epithelium may be the result of <sup>3</sup>H-P8 precipitating in the respiratory epithelium prior to reaching the olfactory epithelium. IV administration resulted in greater systemic (liver and kidney) exposure (0.38  $\mu$ M and 12.5  $\mu$ M) compared to IN administration (0.19  $\mu$ M and 0.30  $\mu$ M). Peak blood concentrations were more than 10 times higher with IV administration (889 nM) compared to IN administration (78 nM). IN delivery of P8 improved brain targeting approximately 4-fold compared to IV delivery, reducing systemic exposure and the risk of potentially unwanted side effects. IN delivery reached the lung in a higher concentration (793 nM) than IV delivery (324 nM); however, the error is very high in the IN group. There were two animals in the IN group (Rats 4 and 10) that had very high concentrations of the peptide in the lungs, possibly the result of <sup>3</sup>H-P8 draining into the lungs from the nasal cavity or the inspiration-inhalation of the IN-dosing solution.

Before averages were calculated, Rat 3 was removed from the study. This was an IV treated animal and the DPMs were much lower than expected in all tissues. The efficiency of IN delivery to the brain was shown to be similar to that reported by Thorne et al. [15], where administration of 5 nmol resulted in 0.5 to 1 nM brain concentrations.

### *Plasma and CSF pharmacokinetics of P8*

In order to ascertain that the radiolabel in the brain indeed represented intact P8 and was not due to leaching or fragmented peptide, an HPLC/MS/MS method for the determination of P8 concentrations in rat plasma and CSF samples was used.

Table 1  
Metabolic stability of P8 in mouse plasma and mouse brain homogenate. Table shows amount of P8 remaining in plasma and brain extract after incubation for 120 mins, expressed as a percentage of P8 at time 0, and half-life of P8.

	Plasma		Brain	
	% of Control at 120 min	Half-Life (min)	% of Control at 120 min	Half-Life (min)
Mouse	100	>240	49.2	120
Human	63.1	>120	51.4	120

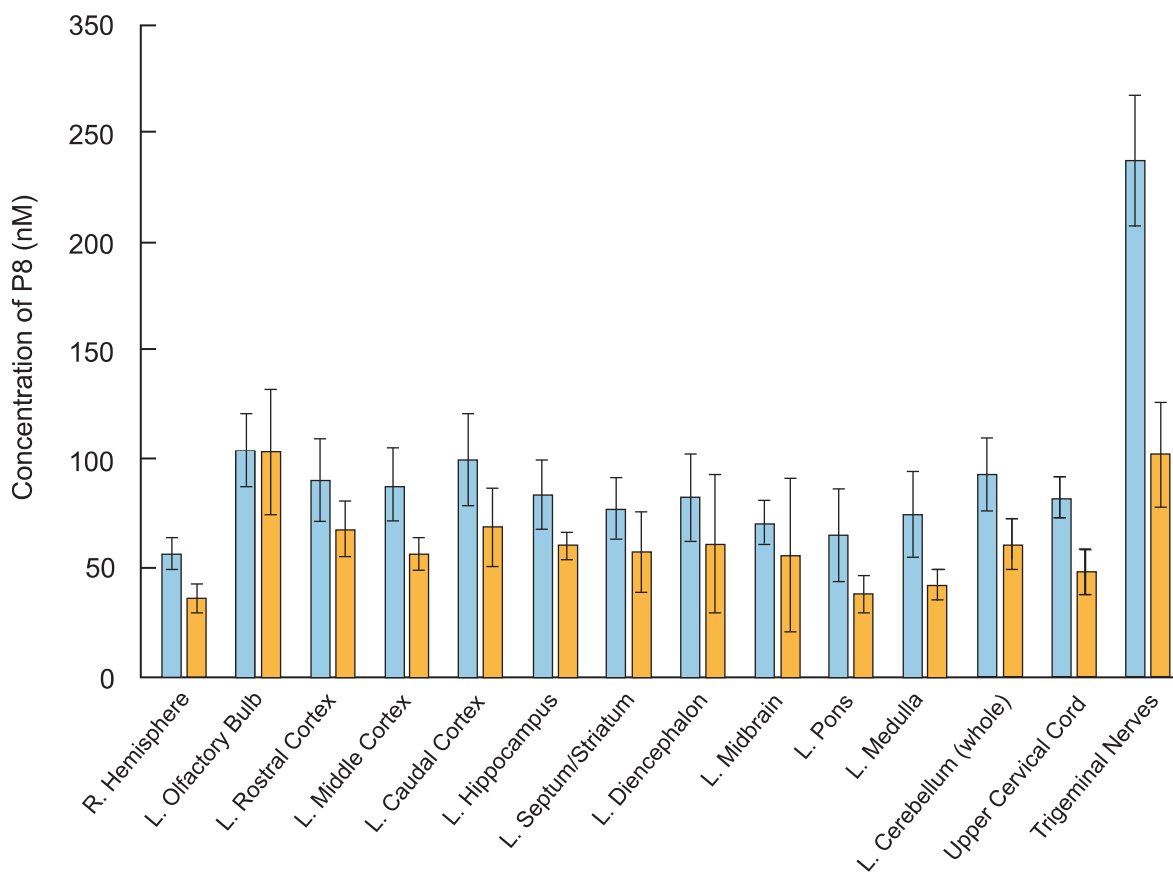


Fig. 2.  $^3\text{H}$ -P8 delivery to brain tissues by intravenous and intranasal administration. Rats ( $n=6$  per dose group) were administered  $^3\text{H}$ -P8 ( $60\ \mu\text{Ci}$ ) and  $0.5\ \text{mg}$  P8 by IN (blue bars) or IV (orange bars) delivery. Brain tissue was collected 30 mins following administration and processed for scintillation counting. Concentration of P8 (nM) was calculated for each brain region and is presented.

Following IV dose administration, P8 exposure was observed with a mean plasma area-under-the-curve (AUC) value of  $679,000 \pm 250,000\ \text{ng}\cdot\text{min}/\text{mL}$  (Tables 3 and 6 and Fig. 3A). This equated to a mean clearance (CL) value of  $17.6 \pm 5.65\ \text{mL}/\text{min}/\text{kg}$ , which is about 25% of hepatic liver blood flow (based on a  $70\ \text{mL}/\text{min}/\text{kg}$  estimate). The volume of distribution was  $0.546 \pm 0.306\ \text{L}/\text{kg}$ , suggesting minimal distribution out of the systemic circulation. The mean terminal half-life ( $t_{1/2}$ ) was  $22 \pm 8.2\ \text{min}$ , which is shorter than the observed plasma stability half-life

in mouse or human. The mean P8 CSF AUC was  $3,270 \pm 226\ \text{ng}\cdot\text{min}/\text{mL}$ , with a peak CSF  $C_{\text{max}}$  value of  $65.6\ \text{ng}/\text{mL}$  observed at the 10-min time point (first time point) (Fig. 3B and Tables 3 and 6). The CSF exposure represents about 0.5% of the observed plasma exposure, however this is likely to be an underestimate as it is unknown what the true peak concentration was in the CSF following IV administration. For both matrices, P8 was still quantifiable at the last time point, suggesting that concentrations were measurable beyond 3 h (Fig. 4A-C).

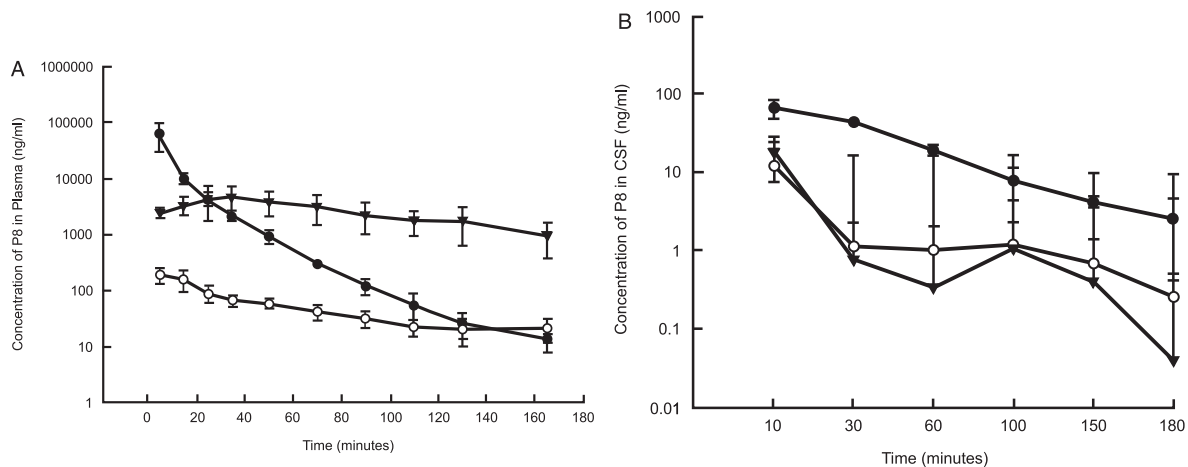


Fig. 3. Mean ( $\pm$ SD) concentrations (ng/ml) of P8 in plasma (A) and CSF (B) of rats following a single IV, IN, or SC dose administration. P8 in PBS (11 mg/kg for IV and SC and 5.5 mg/kg for IN) was delivered to rats ( $n = 6$  per dose group). Blood and CSF samples were removed for up to 180 mins from the onset of administration and analyzed by HPLC as described. PK analysis was performed using standard non-compartmental analysis models in Phoenix WinNonlin (v. 6.3). Black circles: IV administration; Open circles: IN administration; Triangles: SC administration.

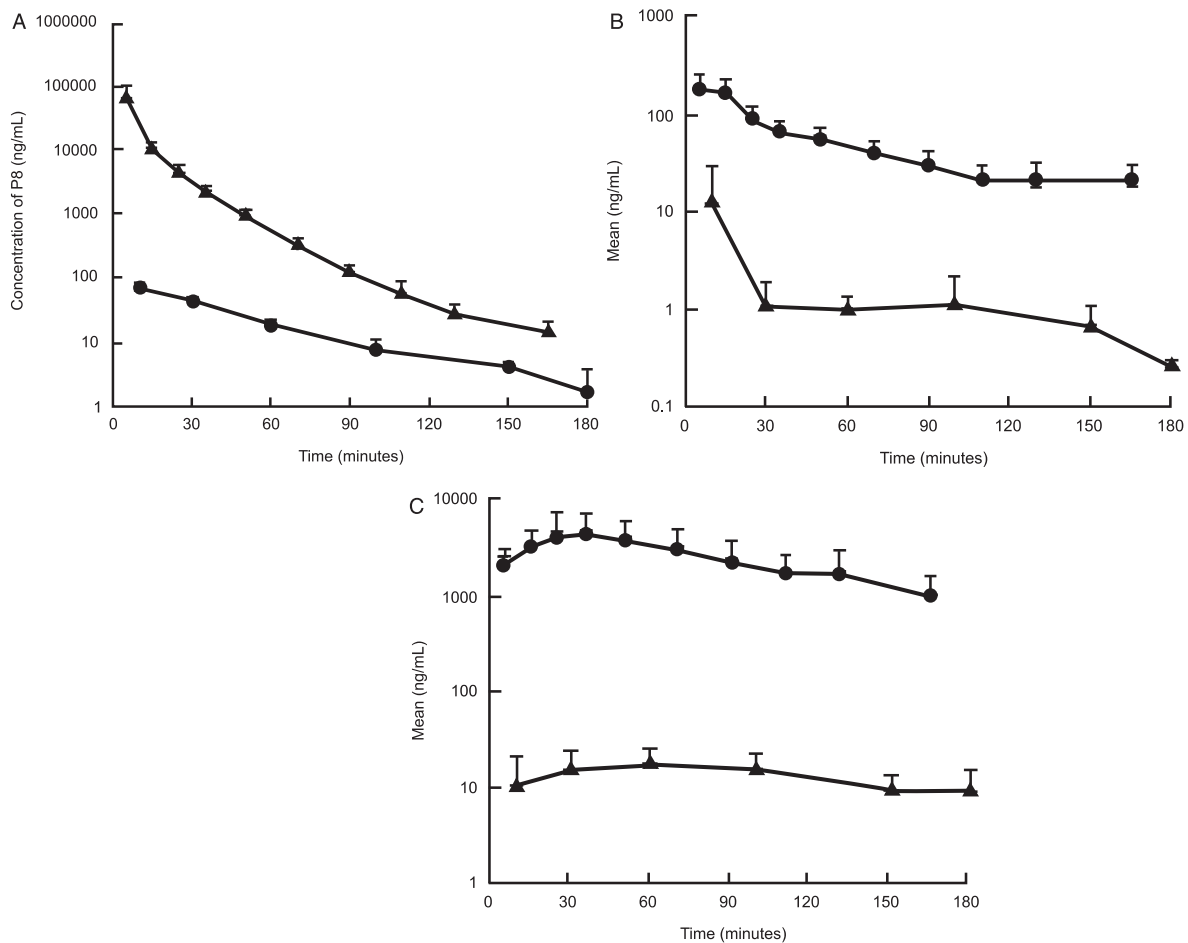


Fig. 4. A comparison of the exposure of P8 in rat plasma and CSF following a single dose IV (A), IN (B), and SC (C) administration. Triangles: Concentration of P8 in plasma; Closed circles: Concentration of P8 in CSF.

Table 2  
Distribution of 3H-P8 in rat plasma and tissues following IV and IN delivery

	IV		IN	
	nM	±Std Dev	nM	±Std Dev
R. Hemisphere	56	7	36	7
L. Olfactory Bulb	104	17	103	29
L. Rostral Cortex	90	19	67	13
L. Middle Cortex	89	17	56	78
L. Caudal Cortex	100	21	68	18
L. Hippocampus	83	16	60	6
L. Septum/Striatum	77	14	57	19
L. Diencephalon	82	20	61	32
L. Midbrain	71	10	56	36
L. Pons	65	22	38	9
L. Medulla	75	20	42	7
L. Cerebellum (whole)	93	17	61	12
Upper Cervical Cord	82	10	48	10
Trigeminal Nerves	238	30	102	24
Olfactory Epithelium	261	51	14,069	11,478
Respiratory Epithelium	279	54	1,303,116	333,108
Lung	324	207	793	1,024
Liver	376	78	188	172
Kidney	12,536	9,826	297	93
10 min Blood Draw	293	299	44	22
20 min Blood Draw	889	427	67	29
30 min Blood Draw	590	346	78	19
Cortex Blood Ratio	0.21	0.1	0.84	0.27

Table 3  
Individual and mean P8 concentrations (ng/mL) in rat plasma and CSF following a single intravenous dose (11.0 mg/kg)

Matrix	Time (min)	Rat I.D.			Mean	SD	
		Rat 1	Rat 2	Rat 3			
Plasma	0	BQL	BQL	BQL	0.00	0.00	
	5	102,000	45,300	43,600	63,600	33,200	
	15	9,880	12,600	8,460	10,300	2,100	
	25	4,250	5,650	3,230	4,380	1,210	
	35	2,160	2,710	1,770	2,210	472	
	50	878	1,190	713	927	242	
	70	392	313	199	301	97.0	
	90	97.3	105	166	123	37.6	
	110	93.1	36.4	39.8	56.4	31.8	
	130	42.0	18.3	20.7	27.0	13.0	
	165	18.9	NSR	9.72	14.3	6.49	
	CSF	0	BQL	BQL	BQL	0.00	0.00
		10	61.1 <sup>c</sup>	50.1 <sup>c</sup>	85.7 <sup>c</sup>	65.6	18.2
30		42.5	48.2 <sup>c</sup>	39.3	43.3	4.51	
60		22.8	17.8	16.9	19.2	3.18	
100		10.7	8.69	4.08	7.82	3.39	
150		4.88	4.30	3.57	4.25	0.656	
180	4.11	NSR	1.06	2.59	2.16		

NSR-No Sample Received.

Following IN dose administration, P8 exposure was observed with a mean plasma AUC value of  $8,780 \pm 1910$  ng-min/mL with a mean  $C_{max}$  value of  $197 \pm 62.7$  ng/mL. The time to peak concentration ( $T_{max}$ ) was 5 min post dose administration, suggesting rapid absorption of P8 (Tables 4 and 6 and Fig. 3A, B). Normalizing the AUC values for the IV and IN routes of administration, the percent of dose absorbed following IN administration was esti-

mated to be about 2.8%. The mean P8 CSF AUC value was  $330 \pm 291$  ng-min/mL with a mean  $C_{max}$  value of  $12.4 \pm 17.7$  ng/mL. The mean CSF  $T_{max}$  value was 26.7 min, suggesting a slower movement into the CSF from the plasma. Following IN administration, the CSF exposure represented about 3.8% of the plasma exposure and was higher than the percent of exposure measured following IV administration. P8 was still quantifiable in the plasma at the last time point sug-

gesting that concentrations were measurable beyond 3 h, whereas for the CSF, the last time point was BLQ (Fig. 4B and Table 4).

Following SC dose administration, P8 exposure was observed with a mean plasma AUC value of  $443,000 \pm 200,000$  ng·min/mL with a mean  $C_{max}$  value of  $5390 \pm 2330$  ng/mL. The time to peak concentration ( $T_{max}$ ) was  $25 \pm 10$  min post dose administration, suggesting slower absorption by the subcutaneous route relative to administration in the nasal cavity. After correcting for the dose administered, the mean plasma exposure was 25-fold higher following SC administration relative to IN administration. A comparison of the SC AUC to the IV AUC showed that the percent of dose absorbed following SC administration was 65%, which as expected, was 25-fold higher than the values observed following IN administration. The mean P8 CSF AUC value was  $2,380 \pm 1,030$  ng·min/mL with a mean  $C_{max}$  value of  $19.8 \pm 8.46$  ng/mL. The mean CSF  $T_{max}$  value was  $43 \pm 29$  min. Following SC administration, the CSF exposure represented about 0.5% of the plasma exposure, which is more consistent with that observed following IV administration (Tables 5 and 6, Fig. 3). Additionally, the plasma concentrations appeared to be more stable and were clearly above the LLOQ at the last measurable time point for both matrices.

#### *Reduction of A $\beta$ in hippocampus of APP transgenic mice following SC administration of P8*

Since the CSF exposure following SC administration represented only  $\sim 0.5\%$  of the plasma exposure, we investigated whether SC administration would provide sufficient amounts of P8 in the brain to reduce A $\beta_{40}$  *in vivo*. Figure 5 shows a reduction in A $\beta_{40}$  in the hippocampus of Tg mice after treatment with P8 for 14 days, showing that the amount of P8 delivered to the brain following SC administration is sufficient to reduce A $\beta$  in this mouse model.

## DISCUSSION

The main findings of the current study presented are that: 1) P8 in its unmodified form is stable, with a half-life in mouse and human plasma of greater than 240 and 120 min, respectively, and a half life in mouse and human brain extracts of 120 min. 2) P8 can be delivered to the brain, CSF, and plasma of rats by IV, IN, and SC administration, as detected by two separate methods. While P8 does cross the blood-brain barrier (BBB), its ratio or relative %F

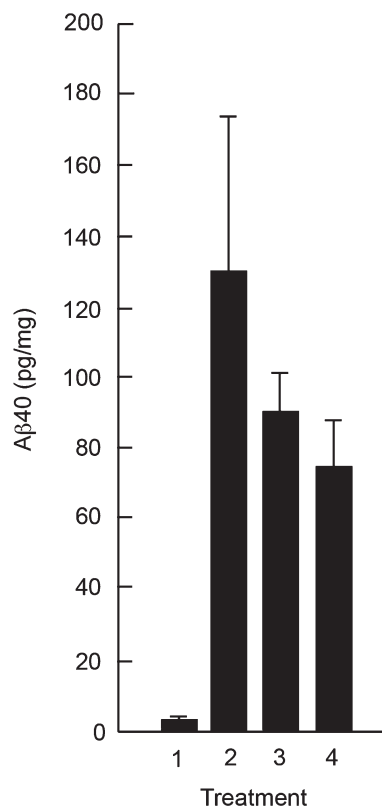


Fig. 5. Reduction of A $\beta$  in hippocampal extracts of APPSWE Tg mice following SC administration of P8. APPSWE Tg mice (2–4) at 16 weeks of age ( $n = 5$  per group) or wild type control mice (1) were administered P8 (3 and 4) or PBS (1 and 2) subcutaneously for 14 days once a day (1–3) or twice a day (4). After sacrifice, A $\beta_{40}$  analysis was performed on hippocampal extracts by ELISA.

is low, being  $<1\%$  of the plasma concentrations, but this amount is sufficient to reduce A $\beta$  in the brains of APP Tg mice. 3) SC administration gave greater absorption of P8 compared to IN and is the delivery method of choice for the further development of P8 as a clinical candidate.

A significant challenge to the development of drug candidates to treat disorders of the CNS is that the systemic delivery of therapeutics to the CNS is not effective for both small and large molecules, due to the presence of the BBB, which prevents their entry to the brain from the circulating blood. The most important factors determining the extent to which a molecule will be delivered from the blood into the CNS are lipid solubility, molecular mass and charge. Therefore, based simply on lipid solubility and molecular mass, any peptide-based neuro-pharmaceutical would almost certainly be impeded by the BBB. Many therapeutic peptides

Table 4

Individual and mean P8 concentrations (ng/mL) in rat plasma and CSF following a single intranasal dose (5.5 mg/kg).  
<sup>c</sup>Below the Quantifiable Limit <0.500 ng/mL; sufficient signal to noise to report as estimates

Matrix	Time (min)	Rat I.D.			Mean <sup>a</sup>	SD <sup>a</sup>	
		Rat 1	Rat 2	Rat 3			
Plasma	0	BQL	BQL	BQL	0.00	0.00	
	5	137	262	191	197	62.7	
	15	102	234	150	162	66.8	
	25	60.8	123 <sup>b</sup>	90.6	91.5	31.1	
	35	53.7	85.9	66.0	68.5	16.2	
	50	66.1	67.7	45.1	59.6	12.6	
	70	37.6	55.3	32.1	41.7	12.1	
	90	32.2	42.8	20.7	31.9	11.1	
	110	26.0	27.0	13.9	22.3	7.29	
	130	33.2	15.0	14.3	20.8	10.7	
	165	32.7	14.9	17.1	21.6	9.70	
	CSF	0	BQL	BQL	BQL	0.00	0.00
		10	0.397 <sup>c</sup>	3.09	32.8	12.1	18.0
30		0.409 <sup>c</sup>	1.03	1.95	1.13	0.775	
60		1.18	0.632	1.28	1.03	0.349	
100		0.537	2.39	0.532	1.15	1.07	
150		0.581	0.372 <sup>c</sup>	1.16	0.704	0.408	
180		0.259 <sup>c</sup>	0.307 <sup>c</sup>	0.225 <sup>c</sup>	0.264	0.0412	

<sup>c</sup>Below the Quantifiable Limit <0.500 ng/mL; sufficient signal to noise to report as estimates.

Table 5

Individual and mean P8 concentrations (ng/mL) in rat plasma and CSF following a single subcutaneous dose (11.0 mg/kg). BQL, Below the Quantifiable Limit <1.00 ng/mL in plasma and <0.500 ng/mL in CSF

Matrix	Time (min)	Rat I.D.			Mean <sup>a</sup>	SD <sup>a</sup>	
		Rat 1	Rat 2	Rat 3			
Plasma	0	BQL	BQL	BQL	0.00	0.00	
	5	3,090	2,420	2,050	2,520	527	
	15	4,790	2,320	3,090	3,400	1,260	
	25	7,740	3,370	2,520	4,540	2,800	
	35	6,790	5,330	2,190	4,770	2,350	
	50	4,860	5,270	1,790	3,970	1,900	
	70	4,360	4,150	1,220	3,240	1,760	
	90	2,600	3,570	908	2,360	1,350	
	110	2,120	2,410	804	1,780	856	
	130	1,870	3,030	619	1,840	1,210	
	165	1,010	1,600	356	989	622	
	CSF	0	BQL	BQL	BQL	0.00	0.00
		10	7.06	22.6	1.75	10.5	10.8
30		25.2	12.8	8.03	15.3	8.86	
60		26.5	17.1	10.3	18.0	8.13	
100		21.6	16.3	8.31	15.4	6.69	
150		11.8	10.7	5.71	9.40	3.25	
180		8.60	15.7	3.18	9.16	6.28	

BQL, Below the Quantifiable Limit <1.00 ng/mL in plasma and <0.500 ng/mL in CSF.

and proteins, in addition, are ineffective when given orally because they are rapidly degraded in the gastrointestinal tract, resulting in a poor PK profile. Nasal delivery of peptides is a non-invasive alternative to invasive delivery methods to by-pass the BBB [16, 17], utilizing pathways along olfactory and trigeminal nerves innervating the nasal passages [18]. IN delivery was therefore initially investigated in the work outlined here as we had not expected P8 to cross the BBB.

Our results showed the unexpected finding that P8 can be delivered to the brain via the blood by both IV and SC delivery more effectively than by IN delivery. These findings were unexpected because even though the size of P8 at 1007 Da is just at the cut-off limit for molecules that can diffuse across the BBB, its net negative charge was considered unfavorable for it to cross the BBB. So how does P8 get to the brain? We can offer a plausible explanation. We know that P8 selectively binds to A $\beta$ PP

Table 6

Summary of mean P8 pharmacokinetic parameters in plasma and CSF from rats following a single IV, IN, or SC dose administration.  $C_{\max}$  is the observed maximum plasma concentration after dosing, units are ng/mL.  $T_{\max}$  is the time  $C_{\max}$  is reached, units are minutes.  $T_{1/2}$  is apparent plasma terminal half-life, units are minutes. AUC is the area under the concentration-time curve from time 0 to the last measurable plasma concentration, units are ng·min/mL. CL is the systemic plasma clearance calculated by the Dose/AUC, units are mL/min/kg. %F is the absolute bioavailability calculated by dividing the dose normalized plasma AUC of route of administration by the dose normalized plasma AUC of the IV dose, multiplied by 100. CSF Ratio is calculated by dividing the dose normalized CSF AUC of the route of administration by the dose normalized CSF AUC of the IV dose

Route	Dose (mg/kg)	Parameter	Matrix		Plasma : CSF Ratio
			Plasma	CSF	
IV	11	CL	17.6 ± 5.65	–	
		$t_{1/2}$	21.9 ± 8.18	–	
		AUC	679,000 ± 250,000	3,270 ± 226	0.0052 ± 0.0015
		Vd, L/kg	0.546 ± 0.306	–	
SC	11	$C_{\max}$	5,390 ± 2,330	19.8 ± 8.46	0.0037 ± 0.0005
		$T_{\max}$	25 ± 10	43 ± 29	
		AUC	443,000 ± 200,000	2,380 ± 1,030	0.0055 ± 0.00054
		%F	65 ± 21		
		CSF Ratio		0.72 ± 0.29	
IN	5.5	$C_{\max}$	197 ± 62.7	12.4 ± 17.7	0.064 ± 0.093
		$T_{\max}$	5.0 ± 0.0	27 ± 29	
		AUC	8,780 ± 1,910	330 ± 291	0.041 ± 0.041
		%F	2.8 ± 0.88		
		CSF Ratio		0.10 ± 0.092	

and does so with high affinity (KD of 3.4 nM) as determined by kinetic studies using biolayer interferometry [13]. One possibility therefore is that P8 from the blood gets translocated across the BBB while still bound to A $\beta$ PP. There are several reports that show the presence of A $\beta$ PP at the endothelial cell membrane [19–21]. It is possible that A $\beta$ PP expressed on the interior face of the endothelial cell of the vessels at the BBB can transport P8 by internalization into endosomes upon peptide binding. As is normal for the brain capillary endothelial cells, the internalized endosomes within these cells may then be transported to the neuronal side of the cells and once across, get released. There are distinct advantages of SC administration over either IV or IN. SC administration requires a simple injection opposed to IV. It is less cumbersome and less expensive than IV. SC administration also requires no special devices as for IN delivery. SC administration delivers a more accurate dose of the drug compared to IN administration; IN administration can also produce irritation of the mucosal membrane. While the %F is <1%, our studies with transgenic mice described herein show that the SC administration of P8 can reduce A $\beta$  levels in the hippocampus and CSF by amounts that were similar to those previously reported [13]. Those latter studies [13] utilized osmotic minipumps to directly administer the peptide to the brain. Studies are ongoing to model the PK/PD relationship in these Tg mice following the SC administration of P8, which will inform future human dosing.

Our current and previously published studies [13] offer the potential for a new, early and effective approach for the treatment of AD, based on a strategy that does not target the secretases. These peptide-induced reductions of total A $\beta$  (and of A $\beta_{40}$  and A $\beta_{42}$ ) do not modify or inhibit either  $\beta$ - or  $\gamma$ -secretase activities. Our approach is therefore very specific and eliminates the numerous off-target effects of the secretase inhibitors while reducing A $\beta$  to very high levels. Our technology is also the earliest in terms of intervention, as it stops the A $\beta$  from being produced, as opposed to dealing with the effects of A $\beta$  once it has accumulated. It is anticipated that these therapeutics will have a significant impact in both treatment and prevention modes and be useful throughout the course of disease.

## ACKNOWLEDGMENTS

This work was supported by NIH grants R43AG043278, R44AG043278 and R43AG055182 to NND.

Individuals or Companies that have assisted in the work: Daniel Dolan, MicroConstants LLC.

Dr. Archie Thurston for discussions and for reviewing the manuscript.

## CONFLICT OF INTEREST

NND has ownership of stocks in Cenna Biosciences Inc and is an author on patent applications

filed by UCSD. Drs. Bruce Morimoto, Marc Azar and David Johnson are employed by separate commercial companies and are consultants for Cenna. Drs. Leah Hanson and William Frey are employed by Health Partners Institute, St. Paul, MN. Neither the companies nor the consultants stand to gain financially or otherwise from this work. They are not a part of the patents or products that may be developed from this work, or part of any grants or gifts. They have no non-financial competing interests, including professional or personal.

## REFERENCES

- [1] Hardy J, Selkoe DJ (2002) The amyloid hypothesis of Alzheimer's disease: Progress and problems on the road to therapeutics. *Science* **297**, 353-356.
- [2] Dawkins E, Small DH (2014) Insights into the physiological function of the  $\beta$ -amyloid precursor protein: Beyond Alzheimer's disease. *J Neurochem* **129**, 756-769.
- [3] Oddo S, Caccamo A, Kitazawa M, Tseng BP, LaFerla FM (2003) Amyloid deposition precedes tangle formation in a triple transgenic model of Alzheimer's disease. *Neurobiol Aging* **24**, 1063-1070.
- [4] Choi YJ, Chae S, Kim JH, Barald KF, Park JY, Lee S-H (2013) Neurotoxic amyloid beta oligomeric assemblies recreated in microfluidic platform with interstitial level of slow flow. *Sci Rep* **3**, 1921-1927.
- [5] Takasugi N, Tomita T, Hayashi I, Tsuruoka M, Niimura M, Takahashi Y, Thinakaran G, Iwatsubo, T (2003) The role of presenilin cofactors in the gamma-secretase complex. *Nature* **422**, 438-441.
- [6] Ahn K, Shelton CC, Tian Y, Zhang X, Gilchrist ML, Sisodia SS, Li Y-M (2010) Activation and intrinsic gamma-secretase activity of Presenilin 1. *Proc Natl Acad Sci U S A* **107**, 21435-21440.
- [7] Lleó A, Saura CA (2011)  $\gamma$ -secretase substrates and their implications for drug development in Alzheimer's disease. *Curr Top Med Chem* **11**, 1513-1527.
- [8] De Strooper B, Annaert W, Cupers P, Saftig P, Craessaerts K, Mumm JS, Schroeter EH, Schrijvers V, Wolfe MS, Ray WJ, Goate A and Kopan R (1999) A presenilin-1-dependent gamma-secretase-like protease mediates release of Notch intracellular domain. *Nature* **398**, 518-522.
- [9] He G, Luo W, Li P, Remmers C, Netzer WJ, Hendrick J, Betayeb K, Flajolet M, Gorelick F, Wennogle LP, Greengard P (2010) Gamma-secretase activating protein is a therapeutic target for Alzheimer's disease. *Nature* **467**, 95-98.
- [10] Kounnas MZ, Danks AM, Cheng S, Tyree C, Ackerman E, Zhang X, Ahn K, Nguyen P, Comer, D, Mao L, Yu C, Pleynt D, Digregorio, PJ, Velicelebi G, Stauderman, KA, Comer WT, Mobley WC, Li YM, Sisodia SS, Tanzi RE, Wagner SL (2010) Modulation of gamma-secretase reduces beta-amyloid deposition in a transgenic mouse model of Alzheimer's disease. *Neuron* **67**, 769-780.
- [11] Fagan T. Liver Tox Ends Janssen BACE program (2018) *Alzheimer Research Forum*, <https://www.alzforum.org/news/research-news/liver-tox-ends-janssen-bace-program>, Posted 18 May 2018, Accessed 21 May 2018.
- [12] Egan MF, Kost J, Tariot PN, Aisen PS, Cummings JL, Vellas B, Sur C, Mukai Y, Voss T, Furtek C, Mahoney E, Mozley L, Vandenberghe R, Mo Y, Michelson D (2018) Randomized trial of Verubecestat for mild-to-moderate Alzheimer's disease. *N Engl J Med* **378**, 1691-1703.
- [13] Dewji NN, Singer SJ, Masliah E, Rockenstein E, Kim M, Harber M, Horwood T (2015) Peptides of presenilin-1 bind the amyloid precursor protein ectodomain and offer a novel and specific therapeutic approach to reduce  $\beta$ -amyloid in Alzheimer's disease. *PLoS One* **10**, e0122451.
- [14] Hsiao K, Chapman P, Nilsen S, Eckman C, Harigaya Y, Younkin S, Yang F, Cole G (1996) Correlative memory deficits, A $\beta$  elevation, and amyloid plaques in transgenic mice. *Science* **274**, 99-102.
- [15] Thorne RG, Pronk GJ, Padmanabhan V, Frey WH (2004) Delivery of insulin-like growth factor-1 to the rat brain and spinal cord along olfactory and trigeminal pathways following intranasal administration. *Neuroscience* **127**, 481-496.
- [16] Ross TM, Martinez PM, Renner JC, Thorne RG, Hanson LR, Frey WH 2nd (2004) Intranasal administration of interferon beta bypasses the blood-brain barrier to target the central nervous system and cervical lymph nodes: A non-invasive treatment strategy for multiple sclerosis. *J Neuroimmunol* **151**, 66-77.
- [17] Alcalá-Barraza SR, Lee MS, Hanson LR, McDonald AA, Frey WH 2nd, McLoon LK (2010) Intranasal delivery of neurotrophic factors BDNF, CNTF, EPO, and NT-4 to the CNS. *J Drug Target* **18**, 179-190.
- [18] Crowe TP, Greenlee MHW, Kanthasamy AG, Hsu WH (2018) Mechanism of intranasal drug delivery directly to the brain. *Life Sci* **195**, 44-52.
- [19] Forloni G, Demicheli F, Giorgi S, Bendotti C, Angeretti N (1992) Expression of amyloid precursor protein mRNAs in endothelial, neuronal and glial cells: Modulation by interleukin-1. *Mol Brain Res* **16**, 128-134.
- [20] Kitazume S, Tachida Y, Kato M (2010) Brain endothelial cells produce amyloid  $\beta$  from amyloid precursor protein 770 and preferentially secrete the O-glycosylated form. *J Biol Chem* **285**, 40097-40103.
- [21] d'Uscio LV, He T, Katusic ZS (2017) Expression and processing of amyloid precursor protein in vascular endothelium. *Physiology* **32**, 20-32.